

# A surprising method for polarising antiprotons.

Th. Walcher<sup>1,2</sup>, H. Arenhövel<sup>1</sup>, K. Aulenbacher<sup>1</sup>, R. Barday<sup>1</sup> and A. Jankowiak<sup>1</sup>

<sup>1</sup> Institut für Kernphysik, Johannes Gutenberg-Universität Mainz, D-55099 Mainz, Germany

<sup>2</sup> Laboratori Nazionali di Frascati, Istituto Nazionale di Fisica Nucleare, I-00044 Frascati (Rome), Italy

Received: date / Revised version: date

**Abstract.** We propose a method for polarising antiprotons in a storage ring by means of a polarised positron beam moving parallel to the antiprotons. If the relative velocity is adjusted to  $v/c \approx 0.002$  the cross section for spin-flip is as large as about  $2 \cdot 10^{13}$  barn as shown by new QED-calculations of the triple spin-cross sections. Two possibilities for providing a positron source with sufficient flux density are presented. A polarised positron beam with a polarisation of 0.70 and a flux density of approximately  $1.5 \cdot 10^{10}/(\text{mm}^2 \text{ s})$  appears to be feasible by means of a radioactive  $^{11}\text{C}$  dc-source. A more involved proposal is the production of polarised positrons by pair production with circularly polarised photons. It yields a polarisation of 0.76 and requires the injection into a small storage ring. Such polariser sources can be used at low (100 MeV) as well as at high (1 GeV) energy storage rings providing a time of about one hour for polarisation build-up of about  $10^{10}$  antiprotons to a polarisation of about 0.18. A comparison with other proposals show a gain in the figure-of-merit by a factor of about ten.

**PACS.** 13.88.+e Polarisation in interactions and scattering – 29.20.Dh Storage rings – 29.25.Bx Electron sources – 29.27.Hj Polarised beams

## 1 Introduction

The spin of elementary particles is essential for their symmetry and in the dynamics of their interaction. After better and better experimental methods for polarising a broad range of different particles have been developed in the last decades, experiments with spin variables represent one of the most significant methods for investigations in subatomic physics.

However, the particularly significant case of the antiproton is still not available for experimental investigations due to the lack of a source of polarised antiprotons. Such a source would allow for studies with isospin and spin symmetry in the interaction of nucleons at low, medium and high energies. In order to substantiate this, three fields are mentioned:

### 1. Spectroscopy of hadrons:

The annihilation of antiprotons on protons produces a multitude of final states with two or more mesons (for a summary see [1]). They carry the potential of containing new states, so called exotics, like glue balls or hybrid states composed of quarks and gluons. However, the analysis of the final states is hampered by the need to perform a partial wave analysis which is frequently not unique. The exploitation of spin degrees of freedom for both the projectile antinucleon and the target nucleon would at least halve the contributing amplitudes and increase the significance of the search for exotics considerably.

Furthermore, the study of known states would be more selective making an identification clearer and offer an additional parameter in the decay dynamics.

### 2. Antinucleon-nucleon scattering and reactions:

The same arguments hold for antinucleon-nucleon elastic scattering. These cross sections have been measured from close to threshold up to many GeV. One particularly intriguing aspect is the spin and isospin dependence of the antinucleon-nucleon interaction at low energies. As is well known the nucleon-nucleon and antinucleon-nucleon potentials are connected in the still very successful meson exchange description by the G-parity symmetry. However, whereas it appears that the long range part of the potential is in this way reasonably well described by pion exchange, there is no sensitivity to the short range part attributed to the vector meson exchange, since the annihilation dominates for radii shorter than about 0.8 fm (for summaries see [2,3]). The different spin orientations in the entrance channel close to threshold, where s- and p-wave scattering dominate, will provide sensitivity to vector mesons, i.e. to the short range of the real part of the antinucleon-nucleon interaction.

For the annihilation dynamics the question whether the quark reorientation or the gluonic quark fusion-creation mechanism (OZI rule violation) prevails is not satisfactorily answered. New data with spin degrees of freedom would provide very significant constraints.

### 3. Antinucleon-nucleon interactions at the parton level:

The generalised parton distributions received recently great attention. It appears that the transversity distribution would become accessible in reactions of polarised antiprotons and protons (for a summary see e.g. [4]). Of course, the experimental efforts for such a study would be considerable

beyond the realisation of a polarised antiproton source. Recently the  $\mathcal{PAX}$  collaboration has proposed just such an investigation for the FAIR facility being prepared at GSI, however, without showing an effective method of polarising antiprotons [5].

Though antiprotons are stable all proposals to polarise them have been less than satisfactory so far. Of the many proposals [6] only two possibilities have been considered as possibly feasible. In the first, the Filtex collaboration has considered the different attenuation of the spin components of an initially unpolarised antiproton beam due to the difference of the singlet and triplet scattering cross sections in the interaction with a polarised hydrogen gas target. In a pilot experiment with protons instead of antiprotons at the Test Storage Ring TSR of the Max-Planck-Institute for Nuclear Physics at Heidelberg in 1992 [7,8,9] this collaboration did indeed find a small effect. The rate of polarisation was, however, only  $dP_b/dt = (0.0124 \pm 0.0006)/h$ , a factor of two smaller than expected theoretically. This is interpreted by Meyer [11] as due to the contribution of the polarised electrons in the polarised hydrogen target. Beside the slow polarisation build-up the scheme is questionable for antiprotons since the total annihilation cross section is two times larger than the elastic scattering and most likely little spin dependent meaning that the beam will be quickly reduced in intensity. Additionally, the Coulomb scattering in the hydrogen gas target reduces the beam lifetime greatly.

The second possibility is the spin transfer in the scattering of initially unpolarised nucleons/antinucleons from polarised electrons of a gas target placed in the coasting beam of a storage ring [10]. This idea has been taken up recently [12] and used as the basis for the proposal of the  $\mathcal{PAX}$  collaboration [5]. However, the internal polarised hydrogen gas target will Coulomb scatter the antiproton beam and makes the use of a very large aperture storage ring mandatory. Therefore, it is not easy to characterise the performance of this method with a few numbers. Table 1 tries to transform the presentation of ref. [12] into numbers which can be compared later to the method proposed in this article.

The meaning of the parameters is evident with the exception of the important single particle space charge limit. It has been calculated using the formula for coasting beams of ref. [13]:

$$N_{\max}^{\Delta Q} = 2\pi\varepsilon\beta_{lab}^2\gamma_{lab}^3r_p^{-1}\Delta Q, \quad (1)$$

where  $\beta_{lab} = v_{lab}/c$ ,  $\gamma_{lab} = 1/\sqrt{1-\beta_{lab}^2}$ ,  $r_p = 1.5$  am is the ‘‘classical proton radius’’ and  $\Delta Q$  is the incoherent tune shift/spread. For common reference the value  $\Delta Q = 0.015$ , a value commonly accepted for the operation of storage rings, has been chosen.

The optimisation of these numbers depends on the way the polarised antiprotons would be used in a certain experiment. We have chosen the example of a low energy antiproton polariser ring and the high energy experimental storage ring HESR of the FAIR project at GSI [12] in order to make a direct comparison possible. However, as we shall discuss in section 4.2, the method proposed here can be adapted to many different situations in storage rings at low and high antiproton energies.

As a summary we note that a polariser has to be evaluated by considering

example	IT <sub>a</sub>	IT <sub>b</sub>	IT <sub>c</sub>
$\Psi_{acc}/\text{mrad}$	50	30	10
$\varepsilon/\text{mm mrad}$	500	180	20
T/MeV	39	61	167
p/(MeV/c)	273	344	584
$\beta = v/c$	0.28	0.34	0.53
$N_{max}^{\Delta Q}$	$2.7 \cdot 10^{12}$	$1.5 \cdot 10^{12}$	$0.6 \cdot 10^{12}$
$N_{max}^R$	$3.6 \cdot 10^{10}$	$3.6 \cdot 10^{10}$	$3.6 \cdot 10^{10}$
$\tau_{pol}^{50\%}/\text{hours}$	39.8	13.9	6.3
$\tau_{AP}/\text{hours}$	16.7	4.6	1.2
$N_{pol}^{50\%}$	$3.3 \cdot 10^9$	$1.8 \cdot 10^9$	$1.9 \cdot 10^8$

**Table 1.** Parameters for the polarisation with an internal polarised hydrogen target method (IT) according to ref. [12].  $\Psi_{acc}$  is the acceptance angle of accelerator needed to accept the Coulomb scattered antiprotons,  $\varepsilon = \Psi_{acc}^2 \cdot \beta_{target}$  is the emittance (it is here defined without  $\pi$ ), T is the kinetic energy of the beam, p is the momentum of the beam.  $N_{max}^{\Delta Q}$  is the maximal number of antiprotons allowed by the limit for the incoherent tune shift/spread  $\Delta Q = 0.015$ ,  $N_{max}^R$  is the maximal number of antiprotons injected in one hour determined by the production rate of antiprotons of  $R = 10^7$  p/s.  $\tau_{pol}^{50\%}$  is the time needed to polarise to 50%,  $\tau_{AP}$  the time in which the number of antiprotons decays to the fraction  $1/e$ , and  $N_{pol}^{50\%}$  the number of polarised antiprotons in the ring after  $\tau_{pol}^{50\%}$ .

- the polarisation build-up time,
- the degree of polarisation after this time,
- the number of antiprotons available after this time, and
- the phase space of the polarised antiprotons.

The evident remedy for avoiding the problems of the internal polarised target as Coulomb scattering and the large and expensive accelerator acceptance would be the interaction of a pure electron beam or target with a pure antiproton target or beam, respectively. This idea, considered since the early phase of the Low Energy Antiproton Ring LEAR at CERN, was, however, never thoroughly pursued since reliable calculations of the cross sections for the polarisation transfer adapted to the situation in a storage ring were missing. However, as will be shown in the following section 2 the cross sections for polarisation transfer from the electron to the antiproton (like signs of charges) are dramatically smaller than the ones for positron-antiproton transfer (unlike signs of charges). This means that a polarised positron source of sufficient flux density is needed. In section 3 we demonstrate that several options exist, all meeting or exceeding the required intensity.

The basis of our proposal is a new QED calculation including Coulomb distortions presented in section 2 for systems with like and unlike charge signs [14,15]. It shows that the total polarisation-transfer-cross sections at small energies become very large. However, as will be discussed in some detail in section 4 only the spin-flip part of the cross section can polarise a beam in a storage ring. Therefore the considerations of Horowitz and Meyer [10,11] are not correct since they treat the non-spin-flip part only. This was recently correctly pointed out by Milstein and Strakhovenko [16]. However, as will emerge in section 2.1 the statement of these authors that the spin-flip cross section due to the hyperfine interaction is generally neg-

ligible is not correct. At very small energies this cross section becomes very large if one includes the distortions due to the Coulomb attraction of particles with unlike electric charges.

In principle the polarisation transfer cross sections from electrons to nucleons have been calculated in the framework of QED since a long time [17, 18, 19, 20, 21] and extensively been used for the measurement of the electric form factor of the neutron and proton (see e.g. [22, 23]). However, these calculations are correctly neglecting the spin-flip part, being small for the high energy electrons used for these experiments, and consider the non-spin-flip part in the polarisation transfer only.

After the new calculations of the cross sections have been summarised in section 2 we present in section 3 a discussion of sources of polarised positrons mostly based on a modest extrapolation of existing technologies. They will be shown to suffice for a realistic scheme in storage rings in section 4. In section 5 we discuss the figure-of-merit for the different proposals and design examples.

## 2 Predictions of polarisation transfer cross sections

In this section we will briefly review the main results of a recent calculation of the general polarisation transfer cross section for the scattering of a polarised hadron (proton or antiproton) on a polarised lepton (electron or positron) at low energies with inclusion of Coulomb effects [14, 15].

The general differential cross section for electromagnetic hadron-lepton scattering with initially polarised hadron and lepton into a state of definite final hadron polarisation (all along incoming momentum as  $z$ -axis) without polarisation analysis of the final lepton is given in the c.m. system by

$$\frac{d\sigma_{\lambda_h^f, \lambda_h^i, \lambda_l^i}^h(\theta, \phi)}{d\Omega} = \frac{M_l^2 M_h^2}{8\pi^2 W^2} \times \text{Tr} \left( T^\dagger(\theta, \phi) \rho_f^h(\lambda_h^f) T(\theta, \phi) \rho_i^h(\lambda_h^i) \rho_l^i(\lambda_l^i) \right), \quad (2)$$

where the trace refers to the hadron and lepton spin degrees of freedom. The invariant energy of the hadron-lepton system is denoted by  $W = E_h + E_l$  and the masses of hadron and lepton by  $M_h$  and  $M_l$ , respectively. The nonrelativistic density matrices for the initial and final states of definite spin along the  $z$ -axis have the form

$$\rho_i^{h/l}(\lambda_{h/l}^i) = \frac{1}{2} (1 + \lambda_{h/l}^i \sigma_z^{h/l}), \quad (3)$$

$$\rho_f^h(\lambda_{h/l}^f) = \frac{1}{2} (1 + \lambda_{h/l}^f \sigma_z^{h/l}), \quad (4)$$

and  $\lambda_{h/l}^{i/f} = \pm 1$ . For scattering into a state of definite lepton polarisation without polarisation analysis of the final hadron one has to replace  $\rho_f^h(\lambda_{h/l}^f)$  by  $\rho_l^i(\lambda_l^i)$ .

For the  $T$ -matrix we include the Coulomb charge and the spin-dependent hyperfine interactions. It has the general form

$$T = 4\pi\alpha Z_l Z_h \left( \frac{a_c}{q^2} - d \boldsymbol{\sigma}^h \cdot \boldsymbol{\sigma}^l - \boldsymbol{\sigma}^h \cdot \overleftrightarrow{D}(\theta, \phi) \cdot \boldsymbol{\sigma}^l \right), \quad (5)$$

where  $\alpha$  denotes the fine structure constant,  $\mathbf{q}$  the three-momentum transfer, and  $Z_{h/l}$  the hadron and lepton charge, respectively.

Furthermore, the parameters  $a_c$ ,  $d$ , and the tensor  $\overleftrightarrow{D}$  depend on what kind of approximation is used, i.e.

(i) Plane wave (PW), corresponding to one-photon-exchange:

$$a_c^{PW} = 1, \quad (6)$$

$$d^{PW} = \frac{2}{3} c^{SS}, \quad (7)$$

$$D_{ij}^{PW} = c^{SS} (\hat{q}_i \hat{q}_j - \frac{1}{3} \delta_{ij}), \quad (8)$$

where  $c^{SS} = \mu_h / (4M_l M_h)$  with  $\mu_h$  for the hadron anomalous magnetic moment, and  $\hat{\mathbf{q}}$  denotes the unit vector along  $\mathbf{q}$ .

(ii) Distorted wave approximation for the hyperfine contribution (DW):

$$a_c^{DW} = e^{i\phi_c}, \quad (9)$$

$$d^{DW} = N(\eta_c)^2 d^{PW}, \quad (10)$$

$$D_{ij}^{DW} = \frac{c^{SS}}{4\pi} \int \frac{d^3 r}{r^3} \psi_{\mathbf{p}'}^{C(-)}(\mathbf{r})^* (3\hat{r}_i \hat{r}_j - \delta_{ij}) \psi_{\mathbf{p}}^{C(+)}(\mathbf{r}), \quad (11)$$

where

$$\phi_c(\theta) = -\eta_c \ln(\sin^2(\theta/2)) + 2\sigma_c, \quad (12)$$

$$\sigma_c = \arg(\Gamma(1 + i\eta_c)), \quad (13)$$

denotes the Coulomb phase with

$$\eta_c = -\alpha Z_l Z_h / v \quad (14)$$

as Sommerfeld Coulomb parameter,  $v$  as the relative hadron-electron velocity, and with the normalisation factor

$$N(\eta_c) = \sqrt{\frac{2\pi\eta_c}{e^{2\pi\eta_c} - 1}} e^{i\sigma_c}. \quad (15)$$

of the incoming and outgoing Coulomb scattering wave functions [24]  $\psi_{\mathbf{p}}^{C(\pm)}$ , respectively.

One should note that the tensor  $D_{ij}$  is symmetric and traceless.

Evaluation of the trace in eq.(2) results in the following expression for the cross section [15]

$$\frac{d\sigma_{\lambda_h^f, \lambda_h^i, \lambda_l^i}^h(\theta)}{d\Omega} = (1 + \lambda_h^i \lambda_h^f) S_0(\theta) + \lambda_l^i (\lambda_h^- S_2^-(\theta) + \lambda_h^+ S_2^+(\theta)) + \lambda_h^i \lambda_h^f S_2(\theta), \quad (16)$$

independent of the azimuthal angle  $\phi$ , where  $\lambda_h^\pm = \lambda_h^i \pm \lambda_h^f$  and

$$S_0(\theta) = V \left( \frac{|a_c|^2}{q^4} + 3|d|^2 + |D_{11}^0(\theta)|^2 + |D_{22}^0(\theta)|^2 + |D_{33}^0(\theta)|^2 + 2|D_{13}^0(\theta)|^2 \right), \quad (17)$$

$$S_2^+(\theta) = 2 \frac{V}{q^2} \Re e(a_c^*(d + D_{33}^0(\theta))), \quad (18)$$

$$S_2^-(\theta) = 2V \left( \Re e(d^* D_{33}^0(\theta) - D_{11}^0(\theta)^* D_{22}^0(\theta)) - |d|^2 \right), \quad (19)$$

$$S_2(\theta) = 2V \left( 2\Re e(d^* D_{33}^0(\theta)) - 2|d|^2 - |D_{11}^0(\theta)|^2 - |D_{22}^0(\theta)|^2 - |D_{13}^0(\theta)|^2 \right), \quad (20)$$

with

$$V = \frac{2\alpha^2 Z_l^2 Z_h^2 M_l^2 M_h^2}{W^2}. \quad (21)$$

The unpolarised cross section is obtained by summing over all spin projections and division by four, i.e.

$$\frac{d\sigma_0}{d\Omega_h} = 2S_0. \quad (22)$$

Now we will discuss different aspects of the general expression of eq. (16) in order to analyse and distinguish spin-flip and non-spin-flip contributions to the polarisation transfer. To this end we will consider completely polarised leptons along the  $z$ -axis, i.e.  $\lambda_l^i = \pm 1$ . The non-spin-flip contributions are given by  $\lambda_h^i = \lambda_h^f = \pm 1$

$$\frac{d\sigma_{+,+, \lambda_l^i}^h(\theta)}{d\Omega} = 2(S_0(\theta) + \lambda_l^i S_2^+(\theta)) + S_2(\theta), \quad (23)$$

$$\frac{d\sigma_{-,-, \lambda_l^i}^h(\theta)}{d\Omega} = 2(S_0(\theta) - \lambda_l^i S_2^+(\theta)) + S_2(\theta). \quad (24)$$

Thus in this case, the polarisation transfer is not the result of a hadron spin-flip, but arises from different scattering strength for the two spin orientations determined by the hyperfine interaction. Their difference for  $\lambda_l^i = 1$  is just the quantity

$$P_{zz} \frac{d\sigma_0}{d\Omega_h} = \frac{d\sigma_{+,+, \lambda_l^i}^h(\theta)}{d\Omega} - \frac{d\sigma_{-,-, \lambda_l^i}^h(\theta)}{d\Omega} = 2S_2^+(\theta), \quad (25)$$

which has been considered by Horowitz and Meyer [10]. Although yielding a polarising effect in the differential cross section, it cannot produce a net hadron polarisation for the situation when all scattered particles are collected together with the incoming beam as will be discussed in detail in section 4.1.1. This is different for the genuine spin-flip contribution, i.e.  $\lambda_h^i = -\lambda_h^f = \pm 1$ , which are given by

$$\frac{d\sigma_{-,+, \lambda_l^i}^h(\theta)}{d\Omega} = 2\lambda_l^i S_2^-(\theta) - S_2(\theta), \quad (26)$$

$$\frac{d\sigma_{+,-, \lambda_l^i}^h(\theta)}{d\Omega} = -2\lambda_l^i S_2^-(\theta) - S_2(\theta). \quad (27)$$

We would like to mention that  $d\sigma_{-,+, \lambda_l^i = +}^h/d\Omega$  had to vanish if the total spin projection  $s_z^h + s_z^l$  would be conserved as intuition might suggest. But this is not the case because of the tensor part of the hyperfine interaction in eq. (5). Indeed, inserting the explicit expressions for  $S_2^-$  and  $S_2$ , one finds

$$\frac{d\sigma_{-,+, \lambda_l^i = +}^h}{d\Omega} = 2V \left( |D_{11}^0(\theta) - D_{22}^0(\theta)|^2 + |D_{13}^0(\theta)|^2 \right), \quad (28)$$

which vanishes completely for  $D_{ij}^0 = 0$ . For the other spin-flip contribution one finds

$$\frac{d\sigma_{+,-, \lambda_l^i = -}^h}{d\Omega} = 2V \left( |2d - D_{33}^0(\theta)|^2 + |D_{13}^0(\theta)|^2 \right), \quad (29)$$

which contributes even for vanishing tensor interaction.

It is just the difference of these two spin-flip contributions which leads to a non-zero net hadron polarisation in a storage ring as will be discussed in Section 4.1.

## 2.1 Results for the integrated spin-flip cross sections

Since the relevant quantities for the polarisation build-up in a storage ring are the integrated spin-flip cross sections we have integrated the general polarisation transfer cross section of eq. (16) over the solid angle except for the small region  $\theta < \theta_{min}$ . The minimal scattering angle is determined by the requirement that the impact parameter should not exceed a given value  $b$ , i.e.

$$\theta_{min} = 2 \arctan(\eta_c/l), \quad (30)$$

with the classical angular momentum  $l = pb$ . In detail we derive

$$\begin{aligned} \sigma_{\lambda_h^f, \lambda_h^i, \lambda_l^i}^h &= 2\pi \int_{\theta_{min}}^{\pi} d\cos(\theta) \frac{d\sigma_{\lambda_h^f, \lambda_h^i, \lambda_l^i}^h(\theta)}{d\cos(\theta)} \\ &= (1 + \lambda_h^i \lambda_h^f) \langle S_0 \rangle \\ &\quad + \lambda_l^i (\lambda_h^- \langle S_2^- \rangle + \lambda_h^+ \langle S_2^+ \rangle) + \lambda_h^i \lambda_h^f \langle S_2 \rangle. \end{aligned} \quad (31)$$

The equations corresponding to eqs. (23), (24) and eqs. (26), (27) are

(i) no hadron spin-flip

$$\sigma_{+,+, \lambda_l^i}^h = 2(\langle S_0 \rangle + \lambda_l^i \langle S_2^+ \rangle) + \langle S_2 \rangle, \quad (32)$$

$$\sigma_{-,-, \lambda_l^i}^h = 2(\langle S_0 \rangle - \lambda_l^i \langle S_2^+ \rangle) + \langle S_2 \rangle. \quad (33)$$

(ii) hadron spin-flip

$$\sigma_{-,+, \lambda_l^i}^h = 2\lambda_l^i \langle S_2^- \rangle - \langle S_2 \rangle, \quad (34)$$

$$\sigma_{+,-, \lambda_l^i}^h = -2\lambda_l^i \langle S_2^- \rangle - \langle S_2 \rangle. \quad (35)$$

In Figure 1 we show first for the range of higher lab kinetic energies between 10 and 100 MeV the result for the two integrated spin-flip cross sections  $\langle \sigma_{\pm, \lambda, \lambda}^h \rangle$  ( $\lambda = \pm$ ) for both, antiproton and proton electron scattering for  $b = 10^{10}$  fm without, i.e. in PW, and with inclusion of Coulomb effects in the

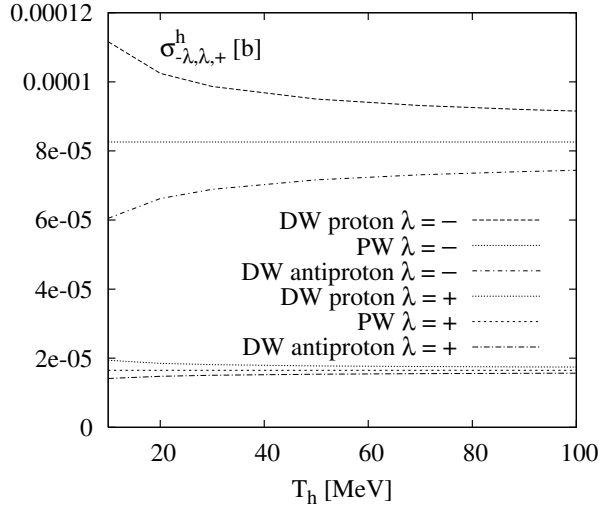


**Fig. 1.** The integrated spin-flip cross sections  $\langle \sigma_{-\lambda, \lambda, +}^h \rangle$  ( $\lambda = \pm$ ) for antiproton and proton electron scattering in the c.m. frame as function of the proton lab kinetic energy  $T_h$  for  $b = 10^{10}$  fm in PW and DW.

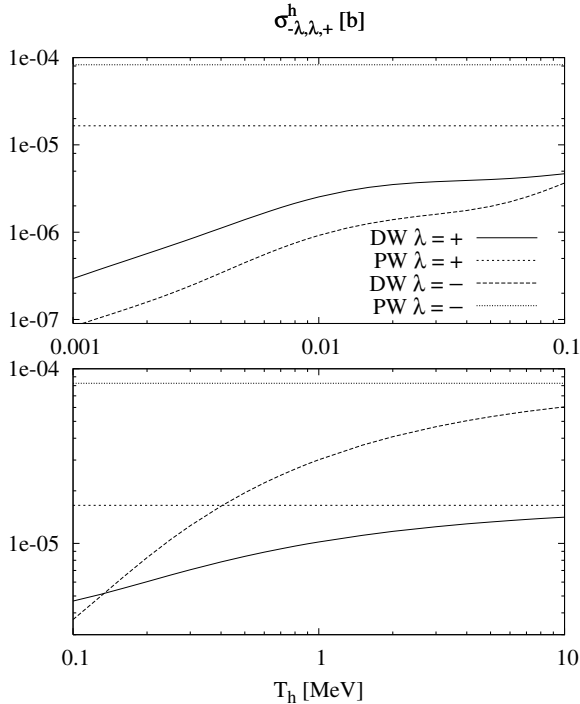


**Fig. 2.** The integrated spin-flip cross sections  $\langle \sigma_{-\lambda, \lambda, +}^h \rangle$  ( $\lambda = \pm$ ) for antiproton electron scattering in the c.m. frame as function of the proton lab kinetic energy  $T_h$  for  $b = 10^{10}$  fm in PW and DW.

distorted wave approximation (DW). One readily notes, that Coulomb effects lead for the proton to an enhancement of the cross sections compared to the PW result due to the attraction of the Coulomb field whereas for the antiproton the repulsion reduces the cross sections. Furthermore, one notes that the

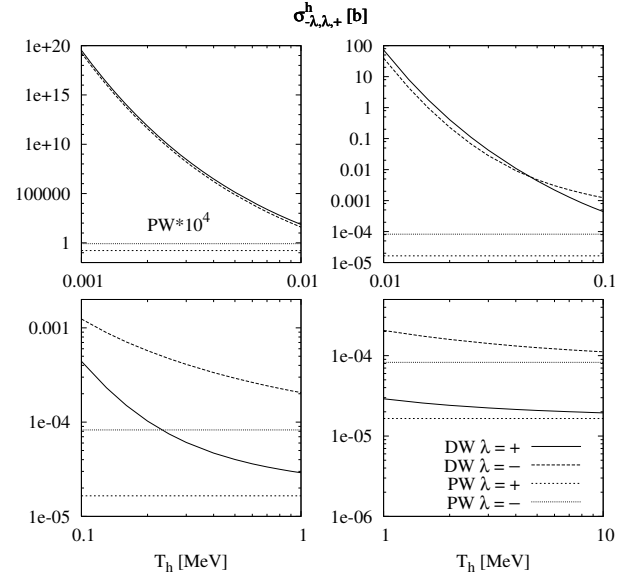


**Fig. 3.** The integrated spin-flip cross sections  $\langle \sigma_{-\lambda, \lambda, +}^h \rangle$  ( $\lambda = \pm$ ) for proton electron scattering in the c.m. frame as function of the proton lab kinetic energy  $T_h$  for  $b = 10^{10}$  fm in PW and DW.

Coulomb influence decreases with increasing kinetic energy, as is to be expected.

The lower energy range between 0.001 and 10 MeV is displayed in Fig. 2 for antiproton electron scattering in PW and DW. It is apparent that below a kinetic energy of 10 MeV Coulomb effects continue to strongly suppress both cross sections, the reduction rapidly increasing with decreasing kinetic energy.

The corresponding results for the proton case are shown in Fig. 3. In contrast to the antiproton case one notes here a very rapid increase of the integrated polarisation cross sections with decreasing energy. This rapid increase is caused essentially by the strong attraction of the Coulomb field pulling in the scattering wave towards small distances. It is governed by a factor  $e^{-2\pi\eta_c}$  (for details see Ref. [14]) which grows very fast with decreasing energy (i.e. increasing  $\eta_c$ ) because for proton electron scattering one has  $\eta_c < 0$ .

Finally, we show in Fig. 4 the ratio  $\langle S_2^- \rangle / \langle S_2 \rangle$  for proton electron scattering which governs the final proton net polarisation (see Section 4).

### 3 Source of polarised positrons

#### 3.1 Direct current (dc) positron source

DC polarised positron beams of narrow energy spread ( $\delta E < 2$  eV) emitted from small source areas ( $A_{\text{source}} = 0.1$  cm<sup>2</sup>) have been developed more than 20 years ago at the University of Michigan [25]. The working principle is angular selective absorption in low  $Z$  absorbers with subsequent moderation in high-purity metal sheets.

The Michigan source was based on a <sup>22</sup>Na emitter ( $\beta^+$  endpoint energy 0.544 MeV) with an activity of 1.7 GBq. The

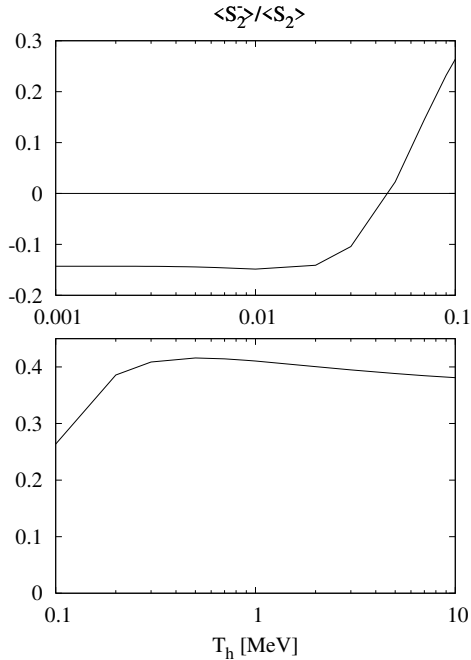


**Fig. 4.** Ratio of  $\langle S_2^- \rangle / \langle S_2 \rangle$  for proton electron scattering in the c.m. frame as function of the proton lab kinetic energy  $T_h$  for DW approximation.

absorption/moderation process limited the beam intensity to  $5 \cdot 10^5 e^+ / s$  with a polarisation of  $P_{e^+} = 0.48$ . The moderator efficiency depends on the absence of positron trapping in defect sites in the bulk of the moderator.

Moderator efficiencies which are larger by more than two orders of magnitude have been obtained by using laser annealed thin tungsten foils in ultra high vacuum [26]. Furthermore, the source activity can be increased by on-line radio-isotope production with a dedicated ion accelerator.

A suitable candidate isotope is  $^{11}\text{C}$  which is produced by the  $^{14}\text{N}(p, \alpha)^{11}\text{C}$  reaction. Typical saturation yields from a Nitrogen gas target are  $8 \text{ GBq} / \mu\text{A}$  at a proton energy of  $18 \text{ MeV}$  [27]. Proton linear accelerators achieving more than  $1 \text{ mA}$  in the desired energy range are commercially available [28]. Therefore, a source activity of  $10^{13} \text{ Bq}$  seems to be achievable at reasonable investment and operating costs. This means that the introduction of improved moderators and online radioisotope production will allow an increase of the positron intensity by six orders of magnitude compared to the Michigan source.

One can make use of this increased intensity to obtain lower positron beam emittance and higher polarisation in the following way: The activity will be extracted and deposited onto a source area of about  $0.3 \text{ mm}$  diameter. In addition it seems advisable to increase beam polarisation by stronger selective absorption. Due to the larger  $\beta^+$  endpoint energy of  $^{11}\text{C}$  ( $1.0 \text{ MeV}$  versus  $0.544 \text{ MeV}$  for the vast majority of the positrons emitted by  $^{22}\text{Na}$ ) and the increased selective absorption we expect an increase of beam polarisation towards  $P_{e^+} = 0.7$ . We believe that the losses inflicted by these two measures will reduce the overall gain with respect to the Michigan design from  $10^6$  to  $10^4$  yielding an intensity of  $5 \cdot 10^9 e^+ / s$ .

An advantageous feature of moderated positrons is their very low energy spread. Positron beam temperatures of less than  $100 \text{ K}$  have been observed when the moderator was cooled to  $23 \text{ K}$  [29]. Since the normalised beam emittance scales  $\propto \sqrt{T}$  a much smaller emittance per emitting area compared to a thermionic (electron) cathode can be obtained. The geometric emittance of the polarised positron beam generated from the  $0.3 \text{ mm}$  diameter spot at the surface will therefore approach the emittance of the cooled antiproton beam (see section 4.2). This means that additional solenoid focusing of the positron beam could then be given up offering complete freedom for choosing the spin direction in the interaction region of positrons and antiprotons. Since the initial energy of the positron beam is very low the desired spin orientation of the positrons can be obtained with very compact spin manipulators as already demonstrated by the Michigan group. Following the spin manipulation an electrostatic post-accelerator will provide the kinetic energies which are required for the two design examples presented in Table 2.

### 3.2 Pulsed positron source with a storage ring

A more effective use of polarised positrons can be made by injecting them as a pulse into a low energy storage ring. Low energy lepton storage rings have already been proposed [30, 31] and are expected to work stably for several seconds at currents of many mA. In order to achieve single turn injection the pulse length should be well below the revolution time. For our purposes we assume a revolution time of  $50 \text{ ns}$  corresponding to  $14 \text{ m}$  circumference for stored positrons of  $1 \text{ MeV}$  kinetic energy. As will be discussed in section 4.2 the momentum spread of the beams should be  $\pm 1 \cdot 10^{-4}$  setting a limit to the longitudinal acceptance of  $\delta E \delta t < 5 \text{ keV ns}$ .

As is well known longitudinally polarised positrons can be generated by converting circularly polarised bremsstrahlung in a converter target [32]. The polarised bremsstrahlung in turn is produced from impinging a beam of polarised electrons on a bremsstrahl target. Here we propose one scheme working with existing technology and describe it starting from the source of polarised electrons to the injection into the mentioned positron storage ring. In order to make it easier to follow Fig. 5 shows the different stages in the sequence of the following description.

The polarised electrons are produced by photo-exciting a suitable semiconductor heterostructure, e.g. strained GaAs. Operation of such a source with current densities of several  $\text{A/cm}^2$  has already been demonstrated [33, 34]. For reasons which will become clear shortly we need a  $4 \mu\text{s}$  long driver pulse with  $1.7 \text{ A}$  peak current ( $6.8 \mu\text{C}$  or  $4.3 \cdot 10^{13}$  electrons per  $4 \mu\text{s}$ -pulse). The polarisation produced routinely with such sources is  $P_{e^-} = 0.83$ . We choose an electron beam energy of  $23 \text{ MeV}$  which can be generated by a linear rf-accelerator. The mentioned energy and bunch charge parameters have already been demonstrated at CERN using optimised rf-travelling wave structures of rather compact design [35]. A capture efficiency of larger than  $0.75$  was achieved necessitating a peak current of up to  $2.2 \text{ A}$  at the source. As will be discussed later we project a  $28 \text{ Hz}$  repetition rate yielding an average current of  $250 \mu\text{A}$  of polarised electrons which is a factor of two larger than that

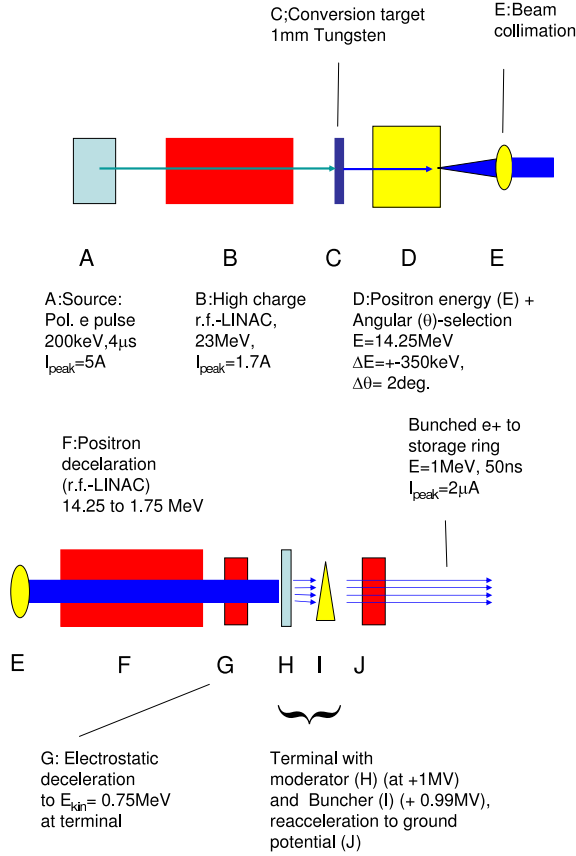


**Fig. 5.** The different stages of the pulsed positron source. A: source of polarised electrons, B: linear electron rf-accelerator for acceleration to 23 MeV, C: combined bremsstrahl and positron production target, D: momentum analyser and solid angle selection, E: focusing into the linear positron rf-decelerator, F: linear positron rf-decelerator, G: electrostatic decelerator, H&I: terminal at +1 MV high voltage with moderator (H) and buncher (I), J: electrostatic accelerator.

of the routine operation at MAMI [36,37], well within reach of ongoing development as discussed below. The  $4\mu\text{s}$  pulse can easily be produced at the source of polarised electrons by gain switching a commercial high power semiconductor laser.

After acceleration the electron beam will be focused on a Tungsten ( $Z = 74$ ,  $A_r = 183.8$ ) bremsstrahl target of 1 mm thickness. From the Bethe-Heitler cross section we estimate for the given peak current of 1.7 A a flux of  $1.2 \cdot 10^{13}$  photons/(4 $\mu$ s-pulse) for the energy interval from 16 to 23 MeV in a cone with a polar angle of  $2^\circ$ . All photons in this interval can produce an electron-positron pair with a total energy of the positron of  $E_+ = (p_+^2 + m_e c^2)^{1/2} = 15.5$  MeV.

As we shall see in section 4.2 we need a good definition of the kinetic energy of the positrons. Therefore, we cut out of the broad positron spectrum a bite of  $\delta p/p_+ = \pm 2.5 \cdot 10^{-2}$  or  $\delta E_+ \approx \delta p_+ = 700$  keV. The design of a suitable beam-handling system allowing this cut poses no problem.

We now use the bremsstrahl target also as conversion target of the circularly polarised photons into longitudinally polarised positrons. The positrons will be produced over the full length of

the target meaning that the effective target thickness is 0.5 mm. Due to collision energy losses these positrons will be decelerated to 14.25 MeV before leaving the target. We extrapolate the differential cross section for the conversion from Fig. 6.12 in ref. [38] for  $\theta_+ = 0^\circ$  in the direction of the photon. We multiply with the momentum bite of 700 keV, the solid angle of  $7.7 \cdot 10^{-3}$  (opening angle of forward cone  $2^\circ$ ), and the photon flux, yielding a peak positron flux of  $8.5 \cdot 10^{10} e^+/(4\mu\text{s-pulse})$ .

So far we have neglected the multiple Coulomb scattering leading to a widening of the positron angular distribution in forward direction. The positrons will be produced over the full length of the target, i.e. an effective target thickness of 0.5 mm. The rms-angle of this distribution can be calculated from the standard formula in ref. [39] to be  $17^\circ$ . Integrating over the  $2^\circ$  cone gives a correction factor of  $6.8 \cdot 10^{-3}$  resulting in  $3.9 \cdot 10^7 e^+/(4\mu\text{s-pulse})$ .

For  $\langle E_\gamma \rangle / E_e \approx 18.5/23$  one gets a degree of polarisation of the photons of 0.95 (see Fig. 5 in ref. [32]). Multiplying this value with the polarisation of the electrons results in 0.79 for the polarisation of the photons. The polarisation of the positrons can now be determined by realising that  $\langle E_+ \rangle / E_\gamma \approx 15.5/18.5 = 0.84$ . From Fig. 5.05 and 5.06 of ref. [38] one reads off  $P_+^L = 0.96$  so that we end with an effective polarisation of the positrons of  $P_{e^+} = 0.76$ . We estimate polarisation losses due to large angle Mott-scattering in the positron production target to be negligible.

However, after passing the momentum selection the positrons still have a energy spread too large to be usable in the positron storage ring. At this stage we can make use of the moderation techniques already discussed for the dc-source in section 3.1. The positrons are decelerated by a further linear accelerator from 15.5 MeV down to about 1.75 MeV and then further to 750 keV by means of a high voltage stage. In the terminal of this high voltage stage we place the moderator. After passing the moderator the positrons are accelerated again up to the optimal kinetic energy needed for the spin transfer. For our example discussed in section 4.2.2 this energy is  $\approx 1$  MeV which the positron beam acquires by leaving the high voltage stage towards ground potential.

The initial transverse momenta are relatively large, thus beam guidance has to be provided in the decelerator by a strong longitudinal solenoid field. For the parameters discussed in the following a solenoid field of 0.5 T suffices. Before entering the decelerator the transverse momenta will be reduced by expanding the beam and collimating it with a suitable lens. Assuming an increase of the beam diameter from initially 2 to 10 mm this will lead to maximum beam angles at the moderator surface of less than  $11^\circ$ . The depolarisation originating from the different orientations of the positron momenta can be neglected. The transverse emittance of the positron beam leaving the moderator will of course be much larger than in the case of the dc-source, but this is partially compensated for by the higher beam energy at the exit. The geometric emittance for the injection into the positron storage ring will therefore be about  $3\pi$  mm mrad. It is important to note that an energy width of less than 0.1 eV is obtained after the moderation resulting in a longitudinal phase space of  $\varepsilon_L \approx 0.4$  keV ns well below the acceptance of the positron storage ring. Before injection the

positron pulse must be compressed in time by a factor of 80 to 50 ns by a bunching system which, however, is not problematic.

Compared to a radioactive  $\beta^+$ -source we find that the decelerated positron beam when hitting the moderator has a similar energy and energy width but is better collimated. We therefore expect that the overall efficiencies for moderation of radioactive sources of about 0.7% [40] can be doubled. Multiplying the total number of highly polarised positrons given above with the estimated moderator efficiency of 0.015 leaves us with  $6 \cdot 10^5 e^+ / (4 \mu\text{s-pulse})$ . It is interesting to note that a very similar positron target has been proposed in ref. [41].

We therefore project the injection of pulses with  $6 \cdot 10^5$  positrons into the low energy storage ring which results in a stored current of  $1.2 \cdot 10^{13} e^+ s^{-1}$  or  $2 \mu\text{A}$ , exceeding the value of the dc-source by a factor of 2000. As will be discussed in detail in the next section the storage ring must be refilled as soon as a considerable fraction of positrons has transferred their polarisation to the antiprotons. Thus a high repetition rate of the driver pulse is demanded for. The limiting factor for the driver rate is the photocathode lifetime. Presently operating conditions at MAMI allow for the extraction of 200C within one lifetime of the photocathode [37] yielding 220 hours of continuous operation for the  $250 \mu\text{A}$  average current required here. Since photocathode regeneration can be obtained within less than two hours by the techniques developed at MAMI [36] it follows that downtime will be negligible.

We have already performed test experiments with average polarised beam currents exceeding 10 mA [42]. These results suggest that operation of a polarised source with sufficiently long lifetime at even an average current of 30 mA is possible. This corresponds to a repetition frequency of 1500 Hz with the same number of positrons per pulse as above. However, one has to optimise the peak current, the repetition frequency, i.e. the average current, and the cathode lifetime. Since this depends on parameters specific for different applications we have not done this optimisation.

If even higher currents of stored polarised positrons are needed one can resort to the more expensive concept of radiative polarisation (Sokolov-Ternov effect) [43]. For the VEPP-2000 project (a storage ring of 4 m radius operating at 1 GeV) it is envisaged to polarise  $10^{11}$  positrons within 12 minutes by radiative polarisation [44]. After polarisation a considerable fraction of the positrons could be decelerated and injected into the low energy storage ring.

## 4 Realisation with a storage ring

After the two essential ingredients, the polarisation-transfer cross sections and the source of polarised positrons have been presented, we want to show how one can build an antiproton polariser based on them. The basic idea is to let the two beams move in parallel with a small relative velocity, i.e. a small relative kinetic energy, and take advantage of the large polarisation-transfer cross section of the leptons to the hadrons in forward direction, making up for the relatively low density of the beam of polarised positrons. (In the following we follow the notation of section 2. Therefore the lepton stands for positron/electron and the hadron for the antiproton/proton, respectively.)

### 4.1 Polarisation build-up

#### 4.1.1 Polarisation build-up with a dc-positron source.

Firstly, we want to calculate the polarisation build-up in an antiproton storage ring using a dc-positron source, the beam of which overlaps with the antiproton beam. We go into the rest frame of the circulating antiproton beam and can use the results of section 2 directly since the cross sections transform as scalars. The quantities in this system are indicated by primes.

Though it is not mandatory for all cases (see section 3) we assume to transport the polarised lepton beam by means of a solenoid with its field in the longitudinal beam direction in order to guarantee a diameter of 2 mm over the full overlap length and to guide the positron beam. Consequently, we chose the quantisation axis (longitudinal spin direction) in the direction of the solenoid field. This means one has to provide a Siberian snake in the ring for rotating the spin longitudinally at the entrance of the solenoid after one circulation.

For the application of eqs. (34) and (35) we have firstly to recall the definition of the polarisation of a particle beam:

$$P_{beam} = \frac{N_+ - N_-}{N_+ + N_-} \quad (36)$$

where  $N_{+/-}$  denotes the number of particles with spin parallel and antiparallel to the polarisation axis, respectively. This definition means that we have to find a difference of the cross sections for the two spin projections along the polarisation axis in a certain kinematical situation. We realise easily that the interactions of case (i) (no spin-flip) cannot polarise the hadron beam in a storage ring. The maximal scattering angle of antiprotons from an electron target is  $\theta'_{max} = m_e/m_p \approx 0.5 \text{ mr}$ . This angle has to be transformed into the ring system giving  $\theta_{max} \ll \theta_{acc}$  where  $\theta_{acc}$  is the acceptance angle of the storage ring. This means that due to the kinematics in the storage ring all particles, whether scattered or not, are recaptured in the beam and, therefore, the polarisation of the coasting beam is unchanged. Another way of looking at this situation is to imagine that the scattered hadrons are “taken out of the beam” [45]. The scattered hadron ensemble is then indeed polarised due to the different cross sections for opposite hadron spin projections under a finite scattering angle in a certain solid angle (see eq. (16)). These hadrons are missing in the hadron beam and leave the beam with a polarisation just, equal but opposite in sign, to the polarisation of the scattered hadrons. Since the scattered hadrons and the remaining beam are not separated geometrically but stay in the coasting beam, no polarisation can be build up on the basis of the cross sections of case (i) in subsection 2.1.

On the other hand, the cross sections of case (ii) in subsection 2.1 are describing a spin-flip, i.e. the hadrons interacting according to these change the spin projection. However, only if the spin-flip is asymmetric for a given lepton polarisation  $\lambda_i^l$  a net polarisation within the coasting beam can be achieved. This is, however, just the case here since

$$\sigma_{-,+, \lambda_i^l}^h \neq \sigma_{+,-, \lambda_i^l}^h. \quad (37)$$

The distinction of case (i) and (ii) in section 2.1 has been obscured in the past by an unfortunate nomenclature. The polarisation transfer, due to the scattering without spin-flip has



been called ‘‘spin transfer’’ [10,11] suggesting spin-flip. The fact that the term  $\langle S_2^+ \rangle$  is not describing spin-flip has been pointed out by Milstein and Strakhovenko [16] as already mentioned in the introduction. In an earlier version the authors of this paper [47] following refs. [10,11] made the same mistake and used their  $\langle P_{zz}\sigma \rangle$  which is the same as the  $d\sigma/d\Omega K_{j00i}$  of ref. [10]. Therefore, as shown in section 2, it is not enough to consider the polarisation transfer, i.e. cross sections with two spin degrees of freedom, but one has to study the triple-spin-cross sections.

We now can proceed and calculate the rate of change of the number of particles with a given hadron spin projection in the ring. First, we consider all quantities in the rest frame of the leptons and indicate them by a prime. We apply the eqs. (34) and (35) to the macroscopic ensemble of the beam in the ring with  $N'_\lambda$  the number of particles of the spin projection  $\lambda$  yielding:

$$\dot{N}'_{-\lambda} = \sigma_{-\lambda,\lambda,\lambda'_i} j_{\lambda'_i}^{\prime\prime} N'_\lambda, \quad (38)$$

where  $j_{\lambda'_i}^{\prime\prime} = n_{\lambda'_i}^{\prime\prime} \beta'_{\text{relative}} c$  is the current density of the lepton,  $n_{\lambda'_i}^{\prime\prime}$  is the lepton density with the spin projection  $\lambda'_i$ , and  $\beta'_{\text{relative}} c$  is the relative velocity of the leptons against the hadrons. For easier notation we introduce the ‘‘helicity’’  $h_{\lambda'_i} = n_{\lambda'_i}^{\prime\prime}/n_0^{\prime\prime}$ , the fraction of leptons of the spin projection  $\lambda'_i$  of the total lepton density  $n_0^{\prime\prime} = n_+^{\prime\prime} + n_-^{\prime\prime}$ . (The helicity is defined in different ways in the literature, but it is convenient to define it here in this way.) We realise that  $h_{\lambda'_i} = (1/2)(1 + \lambda'_i P_l)$  where  $P_l$  is the absolute polarisation of the macroscopic lepton beam.

Now we Lorentz transform eq. (38) to the ring frame indicated by unprimed quantities with  $\beta_{\text{beam}} c$  the velocity of the hadrons in the rest frame of the ring. Firstly, the lepton density is given by  $n_0^{\prime\prime} = n_0^{\prime\prime} \gamma_{\text{beam}}$  due to the length contraction. Secondly, the time dilatation gives a factor of  $1/\gamma_{\text{beam}}$  on the right hand side of eq. (38) cancelling with the previous one. The transformation of the relative velocity  $\beta'_{\text{relative}} c$  gives:

$$\beta'_{\text{relative}} = \frac{\beta_{\text{relative}}}{1 - \beta_{\text{beam}}(\beta_{\text{beam}} \pm \beta_{\text{relative}})} \quad (39)$$

$$\approx \frac{\beta_{\text{relative}}}{1 - \beta_{\text{beam}}^2} = \beta_{\text{relative}} \gamma_{\text{beam}}^2 \quad (40)$$

if  $\beta_{\text{relative}} \ll \beta_{\text{beam}}$ . We also observe that the integrated cross sections are scalars and the same in all reference systems. Further,  $N'_{\lambda h} = N_{\lambda h}$  is conserved.

The rate of eq. (38) has to be multiplied by the ratio of the interaction length  $\ell$  of the lepton beam with the antiproton beam over the circumference of the ring  $L$ . If  $f_h$  is the hadron revolution frequency one has  $\ell/L = f_h \ell / (\beta_{\text{beam}} c)$ . Putting all together eq. (38) reads:

$$\dot{N}_{-\lambda} = \sigma_{-\lambda,\lambda,\lambda'_i} n_0^{\prime\prime} h_{\lambda'_i} f_h \ell \frac{\beta_{\text{relative}}}{\beta_{\text{beam}}} \gamma_{\text{beam}}^2 N_\lambda \quad (41)$$

Since the lepton beam has a finite polarisation we have to add the rates of the two lepton-spin projections:

$$\dot{N}_{-\lambda} = \sum_{\lambda'_i} \sigma_{-\lambda,\lambda,\lambda'_i} h_{\lambda'_i} k_h N_\lambda \quad (42)$$

$$= \kappa_{-\lambda} N_\lambda \quad (43)$$

where

$$k_h = n_0^{\prime\prime} f_h \ell \frac{\beta_{\text{relative}}}{\beta_{\text{beam}}} \gamma_{\text{beam}}^2. \quad (44)$$

We can now write down the overall accounting of the rate of change of spin projections. Since no hadrons are scattered out of the ring  $N_+ + N_- = N_0$  with  $N_0$  the total constant number of hadrons coasting in the ring we have to observe  $\dot{N}_+ = -\dot{N}_-$ . This means we have to subtract from the rate of change of one spin projection the rate of change of the opposite spin projection:

$$\dot{N}_+ = \kappa_+ N_- - \kappa_- N_+ \quad (45)$$

$$\dot{N}_- = \kappa_- N_+ - \kappa_+ N_- \quad (46)$$

with

$$\kappa_+ = (-2\langle S_2^- \rangle P_l - \langle S_2 \rangle) k_h \quad (47)$$

$$\kappa_- = (+2\langle S_2^- \rangle P_l - \langle S_2 \rangle) k_h \quad (48)$$

It is again convenient to introduce the helicities of the hadron beam  $H_+ = N_+/N_0$  and  $H_- = N_-/N_0$  with the beam polarisation  $P_h$  yielding:

$$\dot{P}_h = 2\kappa_+ H_- - 2\kappa_- H_+ \quad (49)$$

From this one finds the differential equation for the beam polarisation build-up

$$\dot{P}_h = (\kappa_+ - \kappa_-) - (\kappa_+ + \kappa_-) P_h \quad (50)$$

with the solution

$$P_h(t) = 2P_l \frac{\langle S_2^- \rangle}{\langle S_2 \rangle} \{1 - \exp[-\kappa_h t]\} - P_h(t=0) \exp[-\kappa_h t] \quad (51)$$

with

$$\kappa_h = 2|\langle S_2 \rangle| k_h. \quad (52)$$

It is evident from these formulae that the maximal polarisation is given by  $P_h^{\text{max}} = 2|P_l \frac{\langle S_2^- \rangle}{\langle S_2 \rangle}|$ . One reads from Fig. 4 the somewhat disappointing  $P_h^{\text{max}} = 0.28$  below 100 keV given by nature. We note that the polarisation build-up is determined by  $\langle S_2 \rangle$  only.

The intense beam of an electron cooler is unpolarised. Since the calculation of the spin-flip cross section cannot be performed at a kinetic energy  $T_h \rightarrow 0$  as given for the cooler, one may worry about the depolarising effect of the cooler. For the antiprotons in focus here, the spin-flip cross sections with electrons are many orders of magnitude smaller due to the Coulomb repulsion (see section 2). Even if we take the maximal cross sections for electrons the achievable current density in electron coolers of about 10 mA/mm<sup>2</sup> yield  $\kappa_{\text{cooler}} \approx 1/(10,000 \text{ h})$  for a realistic storage ring, much too low to produce a noticeable effect. For the proposed test experiments (see section 5), however, this point may have to be considered by switching the cooler on and off. However, the classical limit suggests that  $\langle S_2^- \rangle \rightarrow 0$  for  $T_h \rightarrow 0$ .

#### 4.1.2 Polarisation build-up with a pulsed positron source.

With the dc-positron source we can assume that the polarisation of the lepton beam is constant since it is refed permanently and polarisation loss is negligible by its one path through the interaction region. In the situation of two overlapping storage ring beams, the beams interact for long times. The polarising lepton beam is not anymore a source with constant polarisation, but loses polarisation too and regains polarisation from the hadrons. If left for a sufficiently long time finally an equilibrium between the two beams will occur. However, the point is to refill the lepton ring as often as possible in order to maximise the efficiency. In order to obtain the coupled differential equation for the lepton polarisation it suffices to exchange hadrons and leptons in eq. (50) since the cross sections are invariant under the exchange  $\lambda_f^h \rightarrow \lambda_f^l$ ,  $\lambda_i^h \rightarrow \lambda_i^l$  and  $\lambda_i^l \rightarrow \lambda_i^h$ . We define:

$$k_l = n_0^h f_l \ell \frac{\beta_{\text{relative}}}{\beta_{\text{beam}}} \gamma_{\text{beam}}^2 \quad (53)$$

and get:

$$\dot{P}_h = -4k_h \langle S_2^- \rangle P_l + 2k_h \langle S_2 \rangle P_h = \mu_h P_l - \nu_h P_h \quad (54)$$

$$\dot{P}_l = -4k_l \langle S_2^- \rangle P_h + 2k_l \langle S_2 \rangle P_l = \mu_l P_h - \nu_l P_l \quad (55)$$

The solution of this coupled equations is trivial, but the expressions are lengthy and do not provide much insight. This is inconvenient since the solutions of eqs. (54) and (55) have to be applied iteratively following the numbers of refills of the lepton ring. This means inserting at the beginning of each refill the new initial hadron polarisation and the new initial lepton polarisation and then solve the equations anew. We shall therefore show solutions for the numerical parameters for the design example presented in section 3.2 in graphical form.

## 4.2 Design examples

The different kinds of polarised positron sources offer several applications of polarising antiprotons in storage rings. In this subsection we give two examples of an application of the parallel beam method. The first is a specialised polariser ring together with the dc-source sketched in subsection 3.1. It is optimised for fast polarisation build-up, adequate for an external fixed target experiment requiring a slowly extracted beam. It would be suit for the experiments mentioned in the introduction under “1. Spectroscopy of hadrons” and “2. Antinucleon-nucleon scattering and reactions” in the introduction. The second is the idea to use a small positron storage ring the beam of which overlaps with a storage ring similar to the HESR in ref. [5]. This configuration was already discussed in subsections 3.2 and 4.1.2. It would be suitable for “3. Antinucleon-nucleon interactions at the parton level” in order to allow for a direct comparison of the performance with the scheme presented in ref. [12]. It is, however, not the purpose of this paper to present elaborated proposals. There are too many interlinked parameters and constraints coming from the specific experiments and the accelerator limitations. Some of the limitations and needs for studies in the future will be discussed in section 5.

As discussed in the preceding section 4.1 the decisive cross section for the time needed for polarisation build-up is  $2\langle S_2 \rangle$ . Since we optimise for short times we chose small relative energies between the lepton and hadron. Figure 6 shows the magnification of Fig. 3 suggesting a choice of  $T_h = 0.0017$  MeV yielding  $\langle S_2 \rangle = -2 \cdot 10^{13}$  barn. This choice guarantees the validity of the DW calculation (see refs. [14, 15]) with a large cross section.

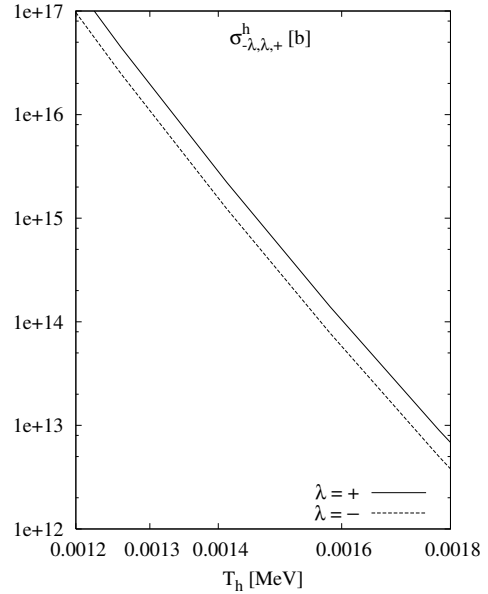


**Fig. 6.** The integrated spin-flip cross sections  $\langle \sigma_{\lambda, \lambda, +}^h \rangle$  ( $\lambda = \pm$ ) for proton electron scattering in the c.m. frame in the region of very low proton lab kinetic energy (magnification from Fig. 3).

### 4.2.1 Specialised polariser ring

First we want to present a specialised polariser ring optimised for fast polarisation build-up. We start with the parameters of the example PB<sub>1</sub> in Table 2 which is close to cooler rings built before, as e.g. LEAR (see [48] and references therein) or the TSR [7]. This design represents a reasonable compromise between size and cost. At the relative kinetic energy of  $T_p = 1.7$  keV we have the ratio  $\langle S_2^- \rangle / \langle S_2 \rangle = -0.143$  (see Fig. 4). If we assume a freely coasting antiproton beam and, in accord with the discussion in subsection 3.1, an average positron current of  $\langle I_e \rangle = 5 \cdot 10^9 e^+ s^{-1}$  and all other parameters as given in Table 2, we get from eq. (44)  $\kappa_h = 2.38 h^{-1}$ . Assuming a positron polarisation of 0.70 we get according to eq. (51) (see Fig. 7) an antiproton polarisation of 0.18 after one hour.

The coasting beam in a storage ring with the parameters assumed for PB<sub>1</sub> in Table 2 represents no problem for the particle dynamics. A few aspects are however mentioned in the following. The incoherent tune shift spread  $\Delta Q$  for our design example is calculated with eq. (1). For  $N^{\Delta Q} = 10^{10}$  we get  $\Delta Q = 0.013$  well in accord with running conditions in existing similar storage rings.  $\Delta Q$  is one of the critical parameters

example	PB <sub>1</sub>	PB <sub>2</sub>
antiproton beam in ring system		
$\beta_{\text{antiproton beam}} = v/c$	0.50	0.95
kinetic energy	145.151 MeV	2066.6 MeV
momentum	541.712 MeV/c	2854.6 MeV/c
rigidity	1.81 T m	9.54 T m
circumference L	75 m	400 m
revolution frequency	2 MHz	0.71 MHz
acceptance	25 $\pi$ mm mrad	
$\beta_0$ at mid overlap	2.2 m	
beam emittance $\pi\varepsilon$	0.45 $\pi$ mm mrad	
beam particles	$10^{10}$	
$\Delta Q_{sp}$	0.014	0.0002
positron beam in ring system		
$\beta_{\text{electron beam}} = v/c$	0.501426	0.950185
kinetic energy	79.6145 keV	1128.47 keV
momentum	295.025 keV/c	1557.80 keV/c
average current $\langle I_e \rangle$	$5 \cdot 10^9 e^+ s^{-1}$	$1.2 \cdot 10^{13} e^+ s^{-1}$
peak current $I_e^{\text{peak}}$	–	$6 \cdot 10^5 e^+ (4 \mu s)^{-1}$
repetition frequency	dc	28 Hz
positron density $n_e$	$1.1 \cdot 10^7 m^{-3}$	$1.4 \cdot 10^{10} m^{-3}$
trans. emittance $\pi\varepsilon_e$	0.45 $\pi$ mm mrad	3 $\pi$ mm mrad
beam diameter	2 mm	
overlap length $\ell$	2 m	
relative motion of electron in antiproton frame		
$\beta'_{\text{relative}}$	0.0019036	
kinetic energy $T_p$	1.7 keV	
kinetic energy $T_e$	0.93 eV	
$\langle S_2 \rangle$	$-2 \cdot 10^{13}$ barn	
$\langle S_2^- \rangle / Sz$	-0.143	
$\tau_{\text{pol.}} = 1/\kappa_h$	0.43 h	6.4 s
$\tau_{\text{pol. build-up}} = \tau_{\text{pbu}}$	1 h	1 h
polarisation $P_l$	0.70	0.76
polarisation $P_h(\tau_{\text{pbu}})$	0.18	0.17

**Table 2.** Two design examples of polarising antiprotons with the parallel beam method (PB) in a storage ring using discussed parameters for the positron sources.  $T_p$  and  $T_e$  are the kinetic energies of the antiproton and positron in the rest frame of the respective other particle.

of the parallel beam method and limits the number of antiprotons in the ring. It may be possible to go to larger  $\Delta Q$  than 0.013 in a specially optimised ring lattice but we did not investigate such an optimisation.

This means that the polariser ring could be filled at the rate of  $10^7 \bar{p}/s$  in about 16 minutes with  $10^{10}$  antiprotons and then polarised in 1 hour, i.e. two polarisation times  $\tau_{\text{pol}} = 1/\kappa_h$ , to a polarisation of 0.18.

The relative kinetic energy 1.7 keV has been chosen to be above the limit of validity of the DWBA calculations. Since the cross sections depend smoothly on the energy no narrow limits

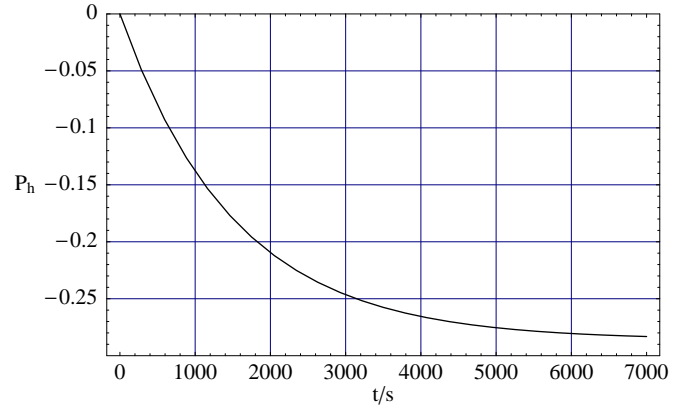


**Fig. 7.** The antiproton polarisation build-up for a polariser with  $P_l = 1$ . and an initially unpolarised hadron beam  $P_h(t=0) = 0$ . The polarisation has to be multiplied by the positron polarisation of 0.7 for the dc source.

are set for the beam spread. Requesting a relative momentum spread of  $\delta p/p = \pm 1 \cdot 10^{-4}$  in the ring system for both the antiproton as well as for the positron, standard in modern storage rings, one arrives after Lorentz transforming at an energy spread of  $\delta T_{\bar{p}} \lesssim |\pm 0.1| T_{\bar{p}} = |\pm 0.17| \text{ keV}$  in the rest system of the electron. These numbers for the following example PB<sub>2</sub> are so similar that they are not discussed separately.

The region of overlap of the antiproton beam and polarised positron beam is assumed to have a length of 2 m. In order to achieve a good efficiency we need a complete overlap with the smallest diameter possible. The diameter we have assumed is 2 mm. As discussed for the dc-source this poses no problem. However, if we want to maintain a diameter for the pulsed source we have to provide a focusing by means of a solenoid. The space charge effects are small and a guiding field of less than 0.01 T suffices to maintain the beam diameter of 2 mm.

For this beam diameter we estimate a minimal value of the beta function  $\beta_{\text{min}}$  of the antiproton beam in mid overlap according to

$$\beta_{\text{min}} = \frac{l/2}{\sqrt{p^2 - 1}}, \quad (56)$$

where  $p = d_e/d_0$  with  $d_e$  the beam diameter at the entrance and exit and  $d_0$  the diameter at the mid point of the overlap region. With  $p = 1.1$  we obtain  $\beta_0 > 2.2$  m. With this value and a beam diameter of 2 mm we get from the relation

$$\sigma_{x,y} = \sqrt{\beta_{x,y} \varepsilon_{x,y}} \quad (57)$$

$\varepsilon_{x,y} = 0.45$  mm mrad as the needed emittance for the antiproton beam. This means that we have to cool the antiproton beam after injection before we can efficiently polarise. The cooling has to stay on during polarisation build-up in order to compensate for the intra-beam scattering and the multiple scattering in the rest gas of the ring. Emittances of about 0.1 mm mrad have been obtained at LEAR and other cooler rings for up to  $10^9$  particles in the ring [48].

#### 4.2.2 HESR as polariser ring

The principle of the dc-source could be used by adjusting the parameters of the previous design example PB<sub>1</sub> to a high energy ring as HESR. On the other hand, the pulsed source offers, as repeatedly mentioned, the interesting option of letting the beam of a positron storage ring overlap with the antiproton beam. This will be investigated in the following.

We start by observing that

$$n_0^l = N_0^l / (A L_l) \quad (58)$$

$$n_0^h = N_0^h / (A L_h) \quad (59)$$

and define:

$$a = \frac{k_l}{k_h} = \frac{(N_0^h / L_h) f_l / \beta_h}{(N_0^l / L_l) f_h / \beta_l} = \frac{N_0^h}{N_0^l} \quad (60)$$

For the parameters collected in Table 2 for the design example PB<sub>2</sub>  $\nu_h = 2k_h | \langle S_2 \rangle | \approx 2 / (6.4 \text{ s})$  and  $a = 1.6 \cdot 10^4$  giving  $\nu_l = a \nu_h \approx 1 / (0.38 \text{ ms})$ . The ratio  $\mu / \nu = 2 \langle S_2^- \rangle / \langle S_2 \rangle$  can be determined with Fig. 4. We plot the solutions of eqs. (54) and (55) with these parameters in Figs. (8), (9), (10), and (11).

We can see that the polarisation build-up gets increasingly inefficient with growing initial polarisation. This is due to the exchange of spin and angular momentum between the hadron and lepton beam. The total spin in the lepton beam is not preserved since the tensor part of the hyperfine interaction transfers spin into angular momentum. For large times both polarisations converge to zero. We also observe that the optimum time, after which the maximum polarisation increase is reached, changes with the number of cycles, i.e. initial polarisation of the hadron beam. It is efficient to stop the polarisation cycle at this optimum time and wait until the lepton source can deliver the next spill for injection into the lepton ring. We show the iterative polarisation build-up as a function of the number of cycles in Fig. 12. If one changes the optimum time from lepton spill to lepton spill one gains somewhat as also shown in Fig. 12.

If we chose  $\delta\tau = 0.2 \text{ ms}$  with a repetition (cycle) time of  $\tau_{cycle} = 36 \text{ ms}$  we get after  $10^5$  cycles a total time for polarisation build up of one hour with a polarisation of  $P_h = 0.22 \cdot P_l(t=0)$ . Considering the polarisation of the positrons  $P_l = 0.76$  we get an effective polarisation of the antiproton beam of 0.17.

It is worth noting that one can use the scheme of this section with a cross section  $\langle S_2 \rangle$  of up to a factor of hundred smaller than predicted by the DW calculation. The time dependence in Figs. 8, 9, 10, and 11 just scales with  $1/Sz$  and the polarisation build-up during one cycle is correspondingly slower. This means that also  $\delta\tau \propto 1/\langle S_2 \rangle$  and one can go up to  $\delta\tau \approx \tau_{cycle}$ . We remind that  $\tau_{cycle}$  is limited by the maximal possible average current of the source of polarised electrons.

## 5 Discussion and Conclusions

Now we want to compare the internal target method (IT) [12] with the parallel beam method (PB) of this article on the basis of the figure-of-merit  $FOM = N_{ob} \cdot P_b^2 / \tau_{pbu}$ , where we mean

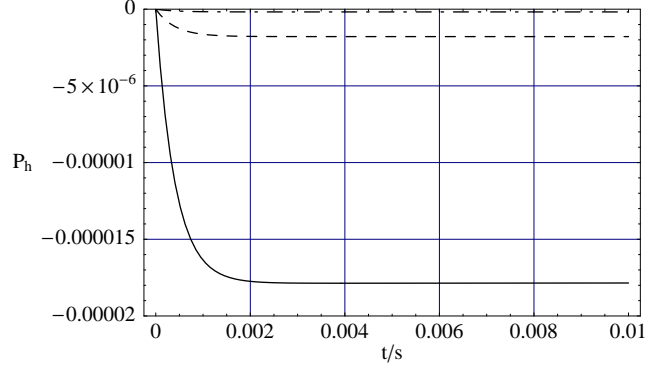


**Fig. 8.** The polarisation build-up  $P_h$  for a single fill with the starting hadron polarisation  $P_h = 0$  and lepton polarisation  $P_l = 1$ . The full curve is for the parameters in Table 2, i.e.  $a = N_0^h / N_0^l = 1.6 \cdot 10^4$ , the dashed curve for  $a = 1.6 \cdot 10^5$ , and the dashed dotted for  $a = 1.6 \cdot 10^6$ .

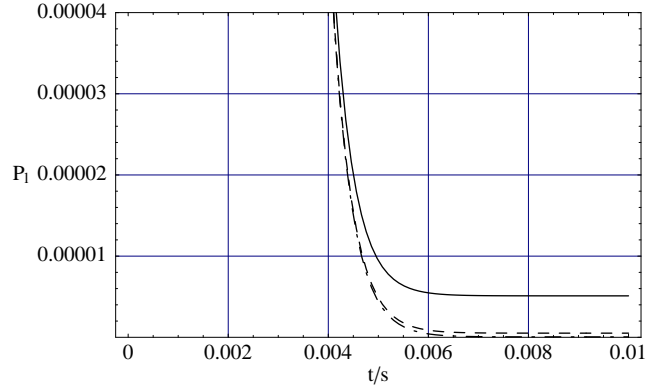


**Fig. 9.** The polarisation build-up  $P_l$  for a single fill with the starting hadron polarisation  $P_h = 0$  and lepton polarisation  $P_l = 1$ . Curves as in fig. 8.

with  $\tau_{pbu}$  the time for one cycle of polarising the antiprotons and using them in an experiment. If the time needed to perform the experiment is shorter or comparable to the polarisation cycle time a reduction of the overall efficiency is indicated which is, however, difficult to reflect in a FOM since it depends on the specific experiment.

For the internal target method we assume a filling time of one hour since it needs many antiprotons in order to make up for the many particles lost due to Coulomb scattering and annihilation. This means that 9 hours are left for polarisation build-up. Further, the numbers of Table 1 are used.

For the parallel beam method PB<sub>1</sub>, i.e. polarisation in a separate polariser ring, we can fill the ring in 16.7 minutes and consequently fill and polarise in one hour. With a polarisation time of  $\tau_{pol.} = 1$  hour we reach a polarisation of the antiprotons of  $P_h = 0.18$ .

For the parallel beam method PB<sub>2</sub> we take as polarisation build-up time  $\tau_{pbu} = 1$  hour using the HESR as polarisation ring. This means that one cannot use the ring for experiments about half of the time assuming a beam life time of two hours in HESR. However, if one would polarise and perform the experiment in parallel, one could do routine detector checks manda-

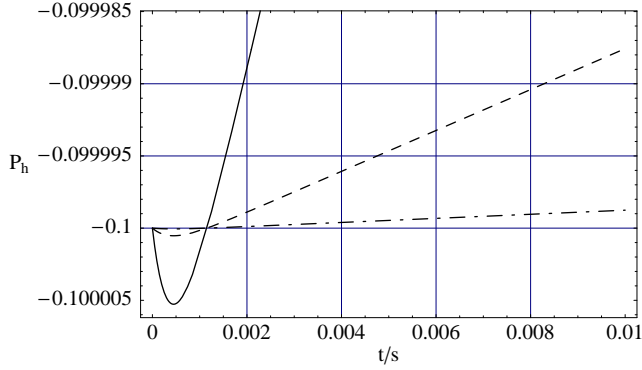


**Fig. 10.** The polarisation build-up  $P_h$  for a single fill with the starting hadron polarisation  $P_h = -0.1$  and lepton polarisation  $P_l = 1$ . Curves as in fig. 8.

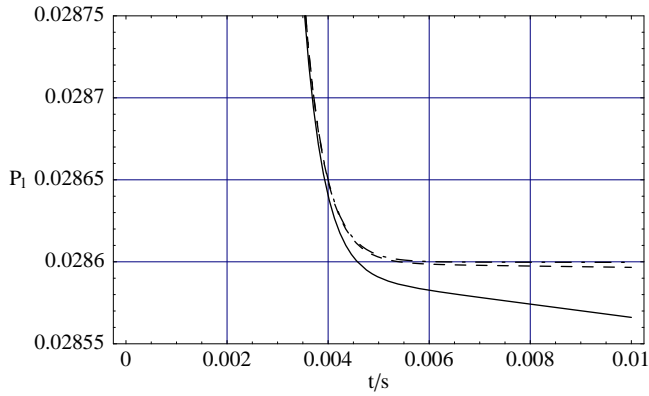


**Fig. 11.** The polarisation build-up  $P_l$  for a single fill with the starting hadron polarisation  $P_h = -0.1$  and lepton polarisation  $P_l = 1$ . Curves as in fig. 8.

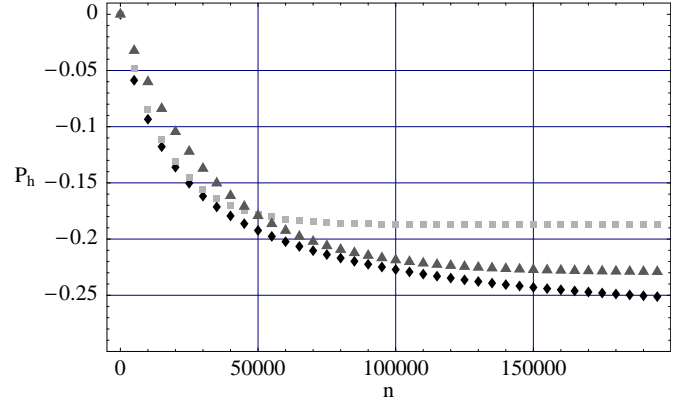
tory for precision measurements in the first half of the life time of small polarisation and do the real experiment in the second half. On the other hand one can easily change the spin direction for the antiprotons with each filling, a feature highly desirable.

Table 3 shows the comparison of all examples. The paral-

method	IT <sub>a</sub>	IT <sub>b</sub>	IT <sub>c</sub>	PB <sub>1</sub>	PB <sub>2</sub>
$N_{pol}$	$2 \cdot 10^{10}$	$5 \cdot 10^9$	$2 \cdot 10^7$	$1 \cdot 10^{10}$	$1 \cdot 10^{10}$
$P_h$	0.11	0.29	0.46	0.18	0.17
$\tau_{pbu} / h$	10	10	10	1	1
FOM	$2.6 \cdot 10^7$	$4.2 \cdot 10^7$	$4.2 \cdot 10^5$	$3.2 \cdot 10^8$	$2.9 \cdot 10^8$

**Table 3.** Figure-of-merit  $FOM = N_b \cdot P_b^2 / \tau_{pbu}$  for the internal target method (IT) with parameters as in Table 1 and for the parallel beam method (PB) with parameters as in Table 2 (see also text). The polarisation for the internal target method has been recalculated using eq. (4) of ref. [12].  $\tau_{pbu}$  is the time needed for one polarisation cycle in an experiment.

lel beam method for polarising antiprotons has figure-of-merits about one order of magnitude better than the internal target method. Unfortunately, the natural limit given by the theoretic-



**Fig. 12.** The polarisation build-up  $P_h$  as a function of the number of lepton refills (cycles) for  $P_h(t = 0) = 0$ ,  $P_l(n \cdot \delta\tau) = 1$ , and  $a = N_0^h / N_0^l = 1.6 \cdot 10^4$ . The polarisation time for one cycle  $\delta\tau$  is 0.4 ms (light grey boxes) and 0.2 ms (dark grey triangles). The black diamonds show a solution for an optimised polarisation time depending on the number of cycles ranging from  $\delta\tau = 1.7$  ms at  $P_h(1) = 0$  for the beginning of the first cycle to  $\delta\tau = 0.16$  ms at  $P_h(6 \cdot 10^4) = -0.2$  for the beginning of the  $6 \cdot 10^4$ th cycle. The cycles repeat with a frequency of 28 Hz in order to limit the average current of the source of polarised electrons.

cally predicted spin-flip cross sections  $\langle S_2 \rangle$  and  $\langle S_2^- \rangle$  does not allow to surpass a maximum polarisation of 0.28. Nevertheless, it appears that the parallel beam method is superior over any other method proposed so far, since it provides a still reasonable polarisation and a large figure-of-merit at low investments. It should be experimentally verified at an existing storage ring as soon as possible in view of the importance for the planning at FAIR. Fortunately the electron-proton interaction has unlike signs as the one of positron-antiproton. If one would inject polarised protons in a storage ring and detune the frequently available electron cooler somewhat one could measure the depolarisation time and determine the spin-flip cross section  $\langle S_2 \rangle$  (see eq. (51) with  $P_l = 0$  and  $P_h(t = 0) \neq 0$ ). However, the spin-flip cross section  $\langle S_2^- \rangle$  can only be determined using polarised leptons. Such a test experiment would completely exclude any risk of an expensive design solely based on the predictions.

This work has been supported by the SFB 443 of the Deutsche Forschungsgemeinschaft (DFG) and the German Federal State of Rheinland-Pfalz.

## References

1. E. Klempt, C. Batty and J.M. Richard, Phys. Rep. **413**, 197 (2005) [arXiv:hep-ex/0501020].
2. Th. Walcher, Ann. Rev. Nucl. Part. Sci. **38**, 67 (1988).
3. E. Klempt, F. Bradamante, A. Martin and J.M. Richard, Phys. Rep. **368**, 119 (2002).
4. V. Barone, A. Drago and P.G. Ratcliffe, Phys. Rep. **359**, 1 (2002) [arXiv:hep-ph/0104283].
5. P. Lenisa and F. Rathmann, Spokespersons of the  $\mathcal{PAX}$  Collaboration, Technical Proposal, Forschungszentrum Jülich 2005, available from www.fz-juelich.de/ikp/pax.

6. Proceedings of the Workshop on Polarized Antiprotons, Edited by A.D. Krisch and O. Chamberlain, Bodega Bay 1985, AIP Conference Proceedings Vol. 145, AIP, New York, 1986.
7. F. Rathmann *et al.*, Phys. Rev. Lett. **71**, 1379 (1993).
8. K. Zapfe *et al.*, Rev. Sci. Instrum. **66**, 28 (1995).
9. K. Zapfe, *et al.*, Nucl. Instrum. Meth. A **368**, 627 (1996).
10. C.J. Horowitz and H.O. Meyer, Phys. Rev. Lett. **72**, 3981 (1994).
11. H.O. Meyer, Phys. Rev. E **50**, 1485 (1994).
12. F. Rathmann, *et al.*, Phys. Rev. Lett. **94**, 014801 (2005).
13. C. Bovet, R. Gourian, I. Gumowski, and K.H. Reich, CERN Report No. CERN/MPS-SI/Int. DL/70/4, 1970.
14. H. Arenhövel, MKPH-T-07-06, submitted to EPJA.
15. H. Arenhövel, to be published
16. A. I. Milstein and V. M. Strakhovenko, Phys. Rev. E **72**, 066503 (2005) [arXiv:physics/0504183].
17. J.H. Scofield, Phys. Rev. **113**, 1599 (1959).
18. J.H. Scofield, Phys. Rev. **141**, 1352 (1966).
19. N. Dombey, Rev. Mod. Phys. **41**, 236 (1969).
20. R.G. Arnold, C.E. Carlson, and F. Gross, Phys. Rev. C **23**, 363 (1981).
21. H. Arenhövel, W. Leidemann and E. L. Tomusiak, Z. Phys. A **331**, 123 (1988).
22. D.I. Glazier *et al.*, Eur. Phys. J. A **24**, 101 (2005) [arXiv:nucl-ex/0410026].
23. C.F. Perdrisat [Jefferson Lab Hall A Collaboration], Eur. Phys. J. A **17**, 317 (2003).
24. A. Messiah, *Mécanique Quantique* (Dunod, Paris 1969).
25. J. Van House and P.W. Zitzewitz, Phys. Rev. A **29**, 96 (1984).
26. F.M. Jacobsen *et al.*, J. Appl. Phys. **67**, 575 (1990).
27. C. VanDeCastele *et al.*, Nucl. Instrum. Meth. A **236**, 558 (1985).
28. A. Nagler *et al.*, Proceedings of LINAC 2006, Knoxville, Tennessee USA, p. 109, <http://epaper.kek.jp/106/PAPERS/MOP033.PDF>.
29. D.A. Fischer *et al.*, Phys. Rev. B **33**, 4479 (1986).
30. I.N. Meshkov, Nucl. Instrum. Meth. A **441**, 255 (2000).
31. I.N. Meshkov, A.O. Sidorin, Nucl. Instrum. Meth. A **391**, 216 (1997).
32. H. Olsen and L.C. Maximon, Phys. Rev. **114**, 887 (1959).
33. R. Alley *et al.*, Nucl. Instrum. Meth. A **365**, 1 (1995).
34. A. Brachmann *et al.*, Proceedings of the 16th International Spin Physics Symposium, SPIN04, Trieste 2004.
35. R. Corsini *et al.*, Proceedings 9th European Accelerator Conference, Lucerne (2004), p. 39.
36. K. Aulenbacher *et al.*, Nucl. Instrum. Meth. A **391**, 498 (1997).
37. K. Aulenbacher *et al.*, Proceedings of the 16th International Spin Physics Symposium, SPIN04, Trieste 2004, Ed. K. Aulenbacher, F. Bradamante, A. Bessan, and A. Martin, World Scientific Publisher, Singapore 2005, p. 975.
38. J. W. Motz, H. A. Olsen and H. W. Koch, Rev. Mod. Phys. **41**, 581 (1969).
39. G. R. Lynch and O I. Dahl, Nucl. Instrum. Meth. B **58**, 6 (1991).
40. P. J. Schultz and K. G. Lynn, Rev. Mod. Phys. **60**, 701 (1988).
41. A. P. Potylitsin, Nucl. Instrum. Meth. A **398**, 395 (1997).
42. R. Barday *et al.*, Proceedings of the 17th International Spin Physics Symposium, Spin06, Kyoto 2006; AIP Conference Proceedings, Vol. 915, 1019 (2007).
43. Y.S. Derbenev and A.M. Kondratenko, Sov. Phys. JETP **37**, 968 (1973).
44. Y. Shatunov, Plans for polarized beams at VEPP-2000; AIP Conference Proceedings, Vol. 915, 153 (2007).
45. N. N. Nikolaev and F. F. Pavlov, arXiv:hep-ph/0601184.
46. N. Nikolaev and F. Pavlov, "Spin filtering of stored (anti)protons: From FILTEX to COSY to AD to FAIR," AIP Conf. Proc. **915**, 932 (2007) [arXiv:hep-ph/0701175].
47. T. Walcher, H. Arenhoevel, K. Aulenbacher, R. Barday and A. Jankowiak, arXiv:0706.3765 [physics.acc-ph].
48. H. Poth, Phys. Rep. **196**, 135 (1990).